Inorganic Chemistry

ARTICLE

pubs.acs.org/IC

Deviation Between the Chemistry of Ce(IV) and Pu(IV) and Routes to Ordered and Disordered Heterobimetallic 4f/5f and 5f/5f Phosphonates

Juan Diwu, Shuao Wang, Justin J. Good, Victoria H. DiStefano, and Thomas E. Albrecht-Schmitt*

Department of Civil Engineering and Geological Sciences and Department of Chemistry and Biochemistry, University of Notre Dame, Notre Dame, Indiana 46556, United States

Supporting Information

ABSTRACT: The heterobimetallic actinide compound $UO_2Ce(H_2O)[C_6H_4(PO_3H)_2]_2\cdot H_2O$ was prepared via the hydrothermal reaction of U(VI) and Ce(IV) in the presence of 1, 2-phenylenediphosphonic acid. We demonstrate that this is a kinetic product that is not stable with respect to decomposition to the monometallic compounds. Similar reactions have been explored with U(VI) and Ce(III), resulting in the oxidation of Ce(III) to Ce(IV) and the formation of the Ce(IV) phosphonate, $Ce[C_6H_4(PO_3H)(PO_3H_2)][C_6H_4(PO_3H)(PO_3)]\cdot 2H_2O$, $UO_2Ce(H_2O)[C_6H_4(PO_3H)_2]_2\cdot H_2O$, and $UO_2[C_6H_4(PO_3H)_2](H_2O)\cdot H_2O$. In comparison, the reaction of U(VI) with Np(VI) only yields $Np[C_6H_4(PO_3H)_2]_2\cdot 2H_2O$ and aqueous U(VI), whereas the reaction of U(VI) with Pu(VI) yields the disordered U(VI)/Pu(VI) compound, $(U_{0.9}Pu_{0.1})O_2[C_6H_4(PO_3H)_2](H_2O)\cdot H_2O$, and the Pu(IV) phosphonate, $Pu[C_6H_4(PO_3H)(PO_3H_2)][C_6H_4(PO_3H)(PO_3)]\cdot 2H_2O$. The reactions of Ce(IV) with Np(VI) yield disordered heterobimetallic phosphonates with both $M[C_6H_4(PO_3H)(PO_3H_2)][C_6H_4(PO_3H)(PO_3)]\cdot 2H_2O$ (M = Ce, Np) and $M[C_6H_4(PO_3H)_2]_2\cdot 2H_2O$ (M = Ce, Np) structures, as well as the Ce(IV) phosphonate $Ce[C_6H_4(PO_3H)(PO_3H_2)][C_6H_4(PO_3H)(PO_3)]\cdot 2H_2O$. Ce(IV) reacts with Pu(IV) to yield the Pu(VI) compound, $PuO_2[C_6H_4(PO_3H)_2](H_2O)\cdot 3H_2O$, and a disordered heterobimetallic Pu(IV)/Ce(IV) compound with the $M[C_6H_4(PO_3H)(PO_3H_2)][C_6H_4(PO_3H)(PO_3)]\cdot 2H_2O$ (M = Ce, Pu) structure. Mixtures of Np(VI) and Pu(VI) yield disordered heterobimetallic Np(IV)/Pu(IV) phosphonates with both the $An[C_6H_4(PO_3H)(PO_3H_2)][C_6H_4(PO_3H)(PO_3)]\cdot 2H_2O$ (M = Np, Pu) and $An[C_6H_4(PO_3H)_2]_2\cdot 2H_2O$ (M = Np, Pu) formulas.

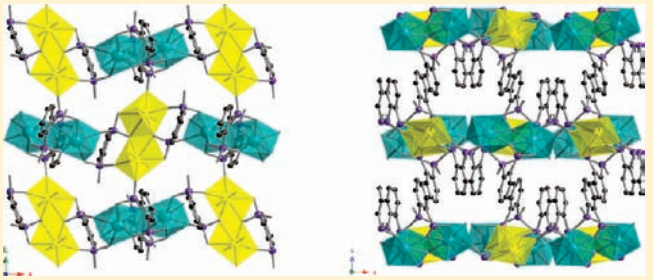

INTRODUCTION

Transuranium elements, especially plutonium, play a special role in advanced technological societies, being responsible for both significant electrical energy production and nuclear weapons arsenals. Activities leading to both of these technologies have resulted in the generation of thousands of tons of high-level nuclear waste that contain transuranium elements in significant quantities.[1−8] Natural thorium and uranium can both be utilized using standard laboratory procedures for working with toxic metals owing to their extremely long half-lives. In contrast, transuranium elements possess much shorter half-lives, and all require specialized facilities, which greatly curtail their availability and the development of their chemistries. One method for circumventing the hazards of transuranium elements is to use elements that potentially mimic their chemistry that are much less dangerous. Using this rationale, Ce(IV) has been used as a surrogate for Pu(IV) owing to its nearly identical ionic radius. U(VI) is used as a replacement for Pu(VI). Th(IV) is used as a substitute for both Np(IV) and Pu(IV). Trivalent lanthanides are used to replace all of the transplutonium elements (e.g., americium and curium) owing to both matching radii and oxidation state. The central question is, do these surrogates mimic the chemistry of transuranium elements sufficiently well that predictions based on their behavior are accurate models of how highly radiotoxic elements will act under key conditions that include long-term storage in repositories, transportation in the environment from contaminated sites, and during necessary separation procedures for recycling used nuclear fuel?

When surrogates are actually compared with transuranium elements, it has been found in many cases that they are not proper mimics of transuranium elements both in solution[9] and in the solid state.[9−13] The foremost example of this that impacts the modeling of plutonium in the environment is that the primary hydrolysis product for U(VI) is a trimer, whereas for Pu(VI), it is a dimer.[13] Raymond and co-workers have demonstrated with both complex octadentate chelating agents and more simple homoleptic chelates of Ce(IV) and Pu(IV) that these two cations can yield substantially different coordination geometries even if

Received: January 3, 2011
Published: April 25, 2011

they possess the same coordination number.[14] Even simple extended structures such as U(VI), Np(VI), and Pu(VI) iodates can yield substantially different structures even if compounds with the same empirical formulas form.[15] Dacheux and company have carefully reviewed the structural chemistry of tetravalent metal phosphates,[16−18] and even in dense structures like $M(PO_3)_4$ (M = Ce, Th, U, Pa, Np, Pu), where one might expect the thermodynamic stability of dense structures to dominate the chemistry, differences among the early actinides and with cerium are observed.[17]

Diphosphonates were selected as a ligand for this study in order to probe potential differences between Ce(IV) and Pu(IV), and the effects of mixing Np(IV) and Pu(IV) with both each other and with Ce(IV). Phosphonates have wide-ranging applications in the nuclear waste remediation and actinide separation processes[19] and are also relevant to the functional groups on the cell walls of the bacteria that are believed to bind actinides under natural conditions.[20,21] In previous reports, we demonstrated that both Np(IV) and Pu(IV) phosphonates and diphosphonates can be prepared via *in situ* hydrothermal reduction of Np(VI) and Pu(VI), which allows for slow kinetics of crystal growth.[22−28] This synthetic methodology is broadly applicable to the crystallization of many tetravalent actinide oxoanion systems.[9−12,22−28] Herein, we disclose routes to both ordered and disordered heterobimetallic 4f/5f and 5f/5f compounds and a rare example of the incorporation of Pu(VI) into a U(VI) material.

EXPERIMENTAL SECTION

Syntheses. Uranyl nitrate $UO_2(NO_3)_2\cdot 6H_2O$ (International Bioanalytical Industries, Inc.), uranyl acetate $UO_2(CH_3COO)_2$ (Fisher Scientific), ammonium cerium nitrate $(NH_4)_2Ce(NO_3)_6$ (Alfa Aesar), cerous nitrate $Ce(NO_3)_3\cdot 6H_2O$ (Matheson Coleman/Bell), and 1, 2-bis(dimethoxyphosphoryl)benzene (Alfa Aesar) were used as received.

$^{237}NpO_2$ (99.9%, Oak Ridge, $t_{1/2} = 2.14 \times 10^6$ years) was prepared via the oxidation of triple electro-refined neptunium metal. ***Caution!*** *^{237}Np represents a serious health risk owing to its α and γ emission.* Specialized facilities and procedures are needed for this work. All free-flowing solids are worked with in negative-pressure gloveboxes, and products are only examined when coated with either water or Krytox oil and water. A 0.372 M stock solution of Np(VI) nitrate was prepare by first digesting NpO_2 in 8 M HNO_3 for 3 days at 200 °C (in an autoclave). The resulting solution was reduced to a residue which oxidizes all of the neptunium to Np(VI). $^{242}PuO_2$ (99.98% isotopic purity, Oak Ridge National Laboratory, $t_{1/2} = 3.76 \times 10^5$ years) was used as received. While the plutonium is of very high isotopic purity, there are trace amounts of ^{238}Pu, ^{240}Pu, ^{241}Pu, ^{244}Pu, and ^{241}Am. The majority of the radioactivity comes from the ^{241}Pu even though it represents only 0.008% of the plutonium. ***Caution!*** *^{242}Pu still represents a serious health risk owing to its α and γ emission.* This isotope was selected because of its long half-life, which increased the longevity of the crystals. A 0.3650 M stock solution of $^{242}Pu(VI)$ nitrate was prepared by first digesting PuO_2 in 8 M HNO_3 for 3 days at 200 °C (in an autoclave). The solution was reduced to a moist residue and redissolved in water. This solution was then ozonated for approximately 5 h to ensure complete oxidation of the plutonium to +6. There are some limitations in accurately determining yield with neptunium and plutonium compounds because this requires weighing a dry solid, which poses certain risks as well as manipulation difficulties given the small quantities with which we work.

$C_6H_4(PO_3H_2)_2$ (PhP2). A total of 10 g of 1,2-bis(dimethoxyphosphoryl)benzene was dissolved in 20 mL of concentrated hydrochloric acid and heated for 30 min followed by refluxing for 8 h. The white crystals of 1,2-phenylenediphosphonic acid (PhP2) formed during cooling to room temperature. The crystals were washed with 10 mL of cold hydrochloric acid, filtered, and finally dried in the oven at 60 °C.[29]

$Ce[C_6H_4(PO_3H)(PO_3H_2)][C_6H_4(PO_3H)(PO_3)]\cdot 2H_2O$ (CePhP2). An alternative preparation is provided for this compound.[28] $Ce(NO_3)_3\cdot 6H_2O$ (0.0418 g, 0.096 mmol) and PhP2 (0.1403 g, 0.5895 mmol) were reacted with 2 mL of distilled water in a 23 mL PTFE autoclave linear. The closed linear was sealed inside a stainless steel autoclave and then heated to 180 °C for three days in a furnace. The furnace was turned off, and the autoclave was allowed to cool to room temperature before opening. The product consisted of pale-yellow acicular crystals of CePhP2.[28]

$U[C_6H_4(PO_3H)_2]_2\cdot 1.5H_2O$ (UPhP2). $UO_2(NO_3)_2\cdot 6H_2O$ (0.1496 g, 0.2980 mmol) and NH_4NO_3 (0.0262 g, 0.3275 mmol) were added to an autoclave along with PhP2 (0.1426 g, 0.5992 mmol). A total of 2 mL of water was then added, and the autoclave was sealed. After heating for 3 days at 220 °C, the reaction mixture was cooled to room temperature by turning off the furnace. The products are pale green acicular crystal of UPhP2 in low yield and some light brown amorphous material.

$(UO_2)_4(H_2O)[C_6H_4(PO_3H)_2][C_6H_4(PO_3H)(PO_3)]_2\cdot 5H_2O$ (UO_2-PhP2-1). $UO_2(NO_3)_2\cdot 6H_2O$ (0.1447 g, 0.2882 mmol) was added to an autoclave along with PhP2 (0.1428 g, 0.6000 mmol). A total of 2 mL of water was then added, and the autoclave was sealed. After heating for 3 days at 180 °C, the reaction mixture was cooled to room temperature by turning off the furnace. The product is yellow acicular crystals of UO_2PhP2-1 in low yield.

$UO_2Ce(H_2O)[C_6H_4(PO_3)(PO_3H)]_2\cdot H_2O$ (UO_2CePhP2). $(NH_4)_2Ce(NO_3)_6$ (0.1436 g, 0.3307 mmol), $UO_2(NO_3)_2\cdot 6H_2O$ (0.1543 g, 0.3074 mmol), and PhP2 (0.1367 g, 0.5744 mmol) were reacted with 2 mL of distilled water in a 23 mL PTFE autoclave linear. The closed linear was sealed inside a stainless steel autoclave and then heated to 180 °C for 3 days in a furnace. The furnace was turned off, and the autoclave was allowed to cool to room temperature before opening. The product consisted of orange acicular crystals of UO_2CePhP2.

$UO_2[C_6H_4(PO_3H)_2](H_2O)\cdot H_2O$ (UO_2PhP2-2). $Ce(NO_3)_3\cdot 6H_2O$ (0.0448 g, 0.1032 mmol), $UO_2(NO_3)_2\cdot 6H_2O$ (0.1516 g, 0.3020 mmol), and PhP2 (0.1429 g, 0.6004 mmol) were reacted with 2 mL of distilled water in a 23 mL PTFE autoclave linear. The closed linear was sealed inside a stainless steel autoclave and then heated to 180 °C for 9 days in a furnace. The furnace was turned off, and the autoclave was allowed to cool to room temperature before opening. The product consisted of pale orange needles of UO_2CePhP2 as the major product along with very pale yellow needles of CePhP2[28] and yellow blocks of UO_2PhP2-2.

$(U_{0.9}Pu_{0.1})O_2[C_6H_4(PO_3H)_2](H_2O)\cdot H_2O$ (UO_2PuO_2PhP2). A 50 μL volume of a 0.365 M stock solution of Pu(VI) was placed in an autoclave along with $UO_2(NO_3)_2\cdot 6H_2O$ (0.0098 g, 0.0195 mmol) and PhP2 (0.0219 g, 0.0920 mmol) in a 10 mL PTFE autoclave linear. They were reacted with 2 mL of distilled water. The closed linear was sealed inside a stainless steel autoclave and then heated to 180 °C for three days in a furnace. The furnace was turned off, and the autoclave was allowed to cool to room temperature before opening. The product consisted of needles of $Pu[C_6H_4(PO_3H)(PO_3H_2)][C_6H_4(PO_3H)(PO_3)]\cdot 2H_2O$ (PuPhP2)[28] as the major product along with large yellow blocks of UO_2PuO_2PhP2 as the minor product.

Reaction of UO_2^{2+} with NpO_2^{2+} and PhP2. A 50 μL volume of a 0.372 M stock solution of Np(VI) was placed in an autoclave along with $UO_2(NO_3)_2\cdot 6H_2O$ (0.0098 g, 0.0195 mmol) and PhP2 (0.0218 g, 0.0916 mmol) in a 10 mL PTFE autoclave linear. They were reacted with 350 μL of distilled water. The closed linear was sealed inside a stainless steel autoclave and then heated to 180 °C for 3 days in a furnace. The furnace was turned off, and the autoclave was allowed to cool to room

dx.doi.org/10.1021/ic200006m |*Inorg. Chem.* 2011, 50, 4842–4850

Table 1. Crystallographic Data for $UO_2Ce(H_2O)[C_6H_4(PO_3)(PO_3H)]_2\cdot H_2O$ ($UO_2CePhP2$), $(UO_2)_4(H_2O)[C_6H_4(PO_3H)_2]$-$[C_6H_4(PO_3H)(PO_3)]_2\cdot 5H_2O$ (UO_2PhP2-1), $UO_2[C_6H_4(PO_3H)_2](H_2O)\cdot H_2O$ (UO_2PhP2-1), $(U_{0.9}Pu_{0.1})O_2[C_6H_4(PO_3H)_2]$-$(H_2O)\cdot H_2O$ (UO_2PuO_2PhP2), $PuO_2[C_6H_4(PO_3H)_2](H_2O)\cdot H_2O$ (PuO_2PhP2), and $U[C_6H_4(PO_3H)_2]_2\cdot 1.5H_2O$ (UPhP2)

compound	$UO_2CePhP2$	UO_2PhP2-1	UO_2PhP2-2	UO_2PuO_2PhP2	PuO_2PhP2	UPhP2
formula mass	912.13	1878.22	538.08	542.05	572.03	730.099
color and habit	orange, acicular	yellow, acicular	yellow, acicular	yellow, acicular	Peach-pink, tablet	Pale-green, acicular
space group	*Pbca*	$P2_1/c$	$P2_1/n$	$P2_1/n$	$P2_1/c$	$P\bar{1}$
a (Å)	15.028(4)	22.316(5)	9.1781(7)	9.168(2)	16.189(2)	7.931(3)
b (Å)	14.959(4)	10.875(2)	7.2095(6)	7.210(2)	7.800(1)	9.961(3)
c (Å)	20.254(6)	17.032(4)	19.323(2)	19.298(4)	12.114(2)	12.952(4)
α (deg)	90	90	90	90	90	99.711(4)
β (deg)	90	103.063(3)	92.073(1)	92.002(4)	108.276(2)	95.693(4)
γ (deg)	90	90	90	90	90	102.967(3)
V (Å^3)	4553(2)	4026.71(15)	1277.7(2)	1274.9(4)	1452.5(4)	972.7(5)
Z	8	4	4	4	4	2
T (K)	100(2)	100(2)	100(2)	100(2)	100(2)	100(2)
λ (Å)	0.71073	0.71073	0.71073	0.71073	0.71073	0.71073
maximum 2*θ* (deg)	27.53	27.60	27.47	28.80	27.15	27.56
ρ_{calcd} (g) cm^{-3})	2.662	3.098	2.797	2.824	2.616	2.493
μ(Mo Kα) (cmP^{-1P})	94.36	163.82	129.97	54.65	48.14	87.43
$R(F)$ for $F_o^2 > 2\sigma(F_o^2)$[a]	0.0377	0.0448	0.0126	0.0147	0.0399	0.0426
$R_w(F_o^2)$[b]	0.0809	0.0902	0.0330	0.0352	0.1018	0.1025

[a] $R(F) = \Sigma||F_o| - |F_c||/\Sigma|F_o|$. [b] $R_w(F_o^2) = [\Sigma[w(F_o^2 - F_c^2)]/\Sigma wF_o^4]^{1/2}$.

temperature before opening. The product consisted of needles of $Np[C_6H_4(PO_3H)_2]_2\cdot 2H_2O$ (NpPhP2)[28] as the major product. UO_2^{2+} remained in solution.

$PuO_2[C_6H_4(PO_3H)_2](H_2O)\cdot H_2O$ (PuO_2PhP2). A 50 μL volume of a 0.365 M stock solution of Pu(VI) was placed in an autoclave along with $(NH_4)_2Ce(NO_3)_6$ (0.0104 g, 0.0190 mmol) and PhP2 (0.0215 g, 0.0903 mmol) in a 10 mL PTFE autoclave linear. They were reacted with 350 μL of distilled water. The closed linear was sealed inside a stainless steel autoclave and then heated to 180 °C for 3 days in a furnace. The furnace was turned off, and the autoclave was allowed to cool to room temperature before opening. The product consisted of needles of $Pu_xCe_{1-x}[C_6H_4(PO_3H)(PO_3H_2)][C_6H_4(PO_3H)$-$(PO_3)]\cdot 2H_2O$ (PuCePhP2) as the major product along with yellow blocks of PuO_2PhP2.

Reaction of Ce^{4+} with NpO_2^{2+} and PhP2. A 50 μL volume of a 0.372 M stock solution of Np(VI) was placed in an autoclave along with $(NH_4)_2Ce(NO_3)_6$ (0.0111 g, 0.0202 mmol) and PhP2 (0.0223 g, 0.0937 mmol) in a 10 mL PTFE autoclave linear. After adding the ligand, the color of the solution changed from pink to green.[23,28] A total of 350 μL of distilled water was then added. The closed linear was sealed inside a stainless steel autoclave and then heated to 180 °C for 3 days in a furnace. The furnace was turned off, and the autoclave was allowed to cool to room temperature before opening. The products were pale green acicular crystals of $Np_xCe_{1-x}[C_6H_4(PO_3H)_2]_2\cdot 2H_2O$ (NpCePhP2) as the major product, an amorphous phase containing Np(VI), and trace amounts of $Np_xCe_{1-x}[C_6H_4(PO_3H)(PO_3H_2)][C_6H_4(PO_3H)(PO_3)]\cdot$ $2H_2O$ (CeNpPhP2) and CePhP2.

Reaction of NpO_2^{2+} with PuO_2^{2+} and PhP2. A 50 μL volume of a 0.365 M stock solution of Pu(VI) and 50 μL volume of a 0.372 M stock solution of Np(VI) along with PhP2 (0.0223 g, 0.0937 mmol) were mixed in a 10 mL PTFE autoclave linear. A total of 350 μL of distilled water was then added. The closed linear was sealed inside a stainless steel autoclave and then heated to 180 °C for 3 days in a furnace. The furnace was turned off, and the autoclave was allowed to cool to room temperature before opening. The products were acicular crystals of $Np_{0.5}Pu_{0.5}[C_6H_4(PO_3H)_2]_2\cdot 2H_2O$ (NpPuPhP2) and $Np_{0.5}Pu_{0.5}[C_6H_4(PO_3H)(PO_3H_2)][C_6H_4(PO_3H)(PO_3)]\cdot 2H_2O$ (PuNpPhP2).

Crystallographic Studies. Crystals of all compounds were mounted on CryoLoops with Krytox oil and optically aligned on a Bruker APEXII Quazar X-ray diffractometer using a digital camera. Initial intensity measurements were performed using an IμS X-ray source, a 30 W microfocused sealed tube (Mo Kα, λ = 0.71073 Å) with high-brilliance and high-performance focusing Quazar multilayer optics. Standard APEXII software was used for determination of the unit cells and data collection control. The intensities of reflections of a sphere were collected via a combination of four sets of exposures (frames). Each set had a different φ angle for the crystal, and each exposure covered a range of 0.5° in ω. A total of 1464 frames were collected with an exposure time per frame of 10−120 s, depending on the crystal. The SAINT software was used for data integration including Lorentz and polarization corrections. Semiempirical absorption corrections were applied using the program SCALE (SADABS).[30] The structures were solved using the SHELX program suite. The heavy atoms were located using direct methods and the least-squares refinement was performed by SHELXL.[31] Selected crystallographic information is listed in Table 1. Atomic coordinates and additional structural information are provided in the Supporting Information (CIFs).

UV−vis−NIR Spectroscopy. UV−vis−NIR data were acquired from single crystals using a Craic Technologies microspectrophotometer. Crystals were placed on quartz slides under Krytox oil, and the data were collected from 400 to 1400 nm. The exposure time was auto-optimized with the Craic software.

Powder X-Ray Diffractometer. Powder patterns were collected from 5° to 80°, with a step of 0.5°, and the data collection time was 0.5 s using a Bruker powder diffractometer with a Lynxeye one-dimensional detector.

SEM/EDS. SEM/EDS images and data were collected using a LEO EVO 50 with an Oxford INCA Energy Dispersive Spectrometer (EDS). Samples were coated with 2 nm of iridium. The energy of the electron beam was 29.02 kV, and the spectrum acquisition time was 120 s. All of the data were calibrated with standards.

dx.doi.org/10.1021/ic200006m |*Inorg. Chem.* 2011, 50, 4842–4850

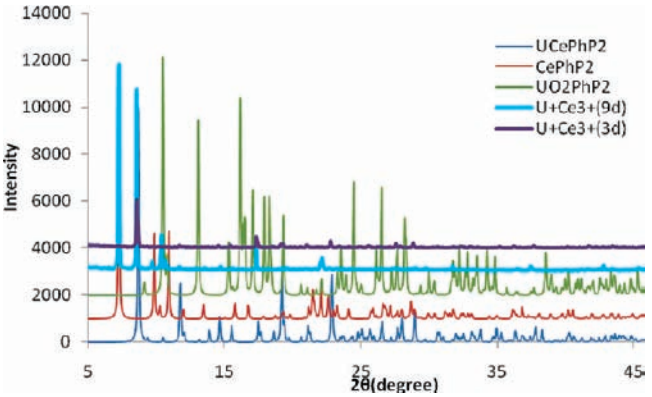

Figure 1. Powder pattern of the U(VI) + Ce(III) reactions showing that the three day reaction only yields $UO_2Ce(H_2O)[C_6H_4(PO_3)(PO_3H)]_2 \cdot H_2O$ ($UO_2CePhP2$), while the nine day reaction gives all three products, $UO_2Ce(H_2O)[C_6H_4(PO_3)(PO_3H)]_2 \cdot H_2O$ ($UO_2CePhP2$), $Ce[C_6H_4(PO_3H)(PO_3H_2)][C_6H_4(PO_3H)(PO_3)] \cdot 2H_2O$ (CePhP2), and $UO_2[C_6H_4(PO_3H)_2](H_2O) \cdot H_2O$ (UO_2PhP2-2).

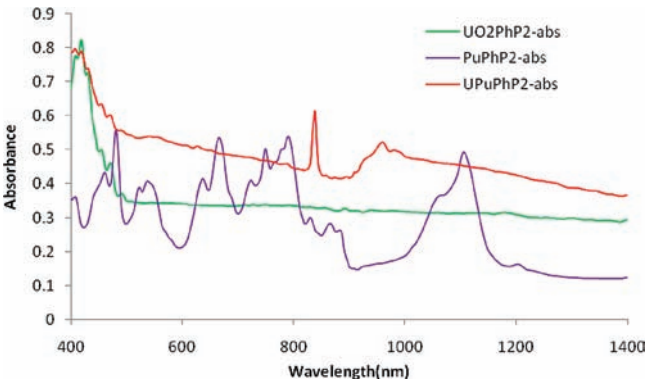

Figure 2. UV−vis−NIR spectra of $UO_2[C_6H_4(PO_3H)_2](H_2O) \cdot H_2O$ (UO_2PhP2-2), $(U_{0.9}Pu_{0.1})O_2[C_6H_4(PO_3H)_2](H_2O) \cdot H_2O$ (UO_2PuO_2-PhP2), and $Pu[C_6H_4(PO_3H)(PO_3H_2)][C_6H_4(PO_3H)(PO_3)] \cdot 2H_2O$ (PuPhP2), showing that there is Pu(VI) in the UO_2PuO_2PhP2 crystal not in UO_2PhP2, and PuPhP2 is a Pu(IV) crystal.

RESULTS AND DISCUSSION

Synthesis. Relatively short-lived transuranium isotopes (e.g., ^{239}Pu, ^{241}Am, ^{243}Am, and ^{249}Cf) produce substantial quantities of radiolysis products that must be utterly ignored in order to propose that surrogates provide reasonable mimics. Even if this is done, there are still large differences in the redox chemistry of these elements. For instance, Ce(IV) is the highest possible oxidation state for cerium, and it is easily reduced to Ce(III) ($E^{\circ}_{Ce(III)/Ce(IV)}$ = 1.61 V). We established in our previous work that Np(IV), which is very difficult to further reduce to Np(III), can be isolated from the precipitation-driven reaction of Np(V) disproportionation.[22−28] Whereas with Pu(IV), which can easily form from the reduction of Pu(VI), the redox potential ($E^{\circ}_{Pu(III)/Pu(IV)}$ = 0.97 V) is considerably smaller than its Ce(IV) counterpart.

The complexation of cerium substantially influences the Ce(III)/Ce(IV) redox couple. In a strong base, it is sufficiently lowered such that oxygen from air oxidizes Ce(III) to Ce(IV). We find a similar effect in the phenylenediphosphonate system. Whether Ce(III) or Ce(IV) is employed in the starting reactions,

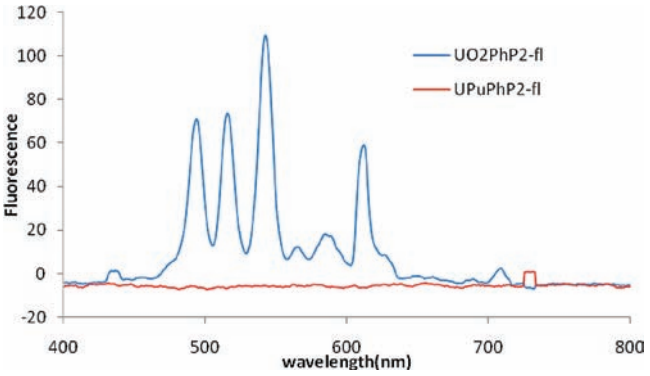

Figure 3. Fluorescence spectra of $UO_2[C_6H_4(PO_3H)_2](H_2O) \cdot H_2O$ (UO_2PhP2-2) and $(U_{0.9}Pu_{0.1})O_2[C_6H_4(PO_3H)_2](H_2O) \cdot H_2O$ (UO_2PuO_2PhP2), showing that, with only 10% of Pu(VI) in the structure, the fluorescence was diminished.

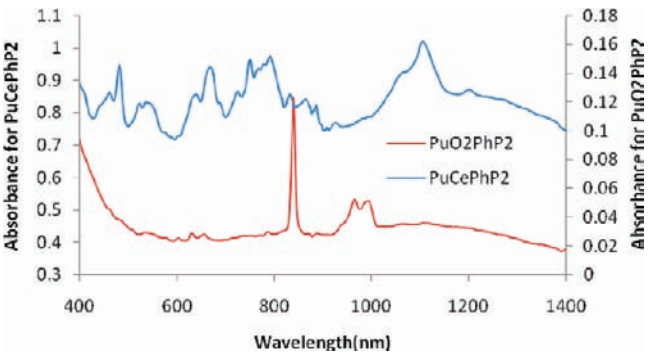

Figure 4. UV−vis−NIR spectra of $Pu_xCe_{1-x}[C_6H_4(PO_3H)(PO_3H_2)][C_6H_4(PO_3H)(PO_3)] \cdot 2H_2O$ (PuCePhP2) and $PuO_2[C_6H_4(PO_3H)_2](H_2O) \cdot H_2O$ (PuO_2PhP2), showing that it is Pu(VI) in the PuO_2PhP2, and Pu(IV) exists in PuCePhP2 crystals.

Ce(IV) is the only oxidation state isolated in the products. This reaction is also driven by the substantially lower solubility of compounds with tetravalent metals versus trivalent metals. Np(VI) and Pu(VI) are always reduced in these same reactions to the tetravalent state. Again, this is probably solubility driven.

Ce(IV) and U(VI) can be combined with phenylenediphosphonate to yield the heterobimetallic compound $UO_2Ce(H_2O)[C_6H_4(PO_3H)_2]_2 \cdot H_2O$. Prolonged heating (nine days) of this compound leads to its decomposition and subsequent formation of the monometallic compounds that contain only U(VI) or Ce(IV). The heterobimetallic, mixed oxidation state compounds are not isolated when U(VI) is combined with Np(VI) and Pu(VI). All of the products isolated only contain a single metal. These studies indicate that the Ce(IV)/U(VI) compound is a kinetically stabilized product that is unstable with respect to decomposition to products that contain only one type of metal. Figure 1 displays the X-ray diffraction powder patterns of the reactions compared with the theoretical patterns of $UO_2CePhP2$, CePhP2, and UO_2PhP2-2, demonstrating that multiple products exist in reactions with nine day durations. It is important to note however that the crystallization of $UO_2[C_6H_4(PO_3H)_2](H_2O) \cdot H_2O$ acts as a carrier of Pu(VI), and 10% of the U(VI) is replaced by Pu(VI), yielding $(U_{0.9}Pu_{0.1})O_2[C_6H_4(PO_3H)_2](H_2O) \cdot H_2O$. This is demonstrated by both EDS and UV−vis−NIR spectroscopy, the former providing a

dx.doi.org/10.1021/ic200006m |Inorg. Chem. 2011, 50, 4842–4850

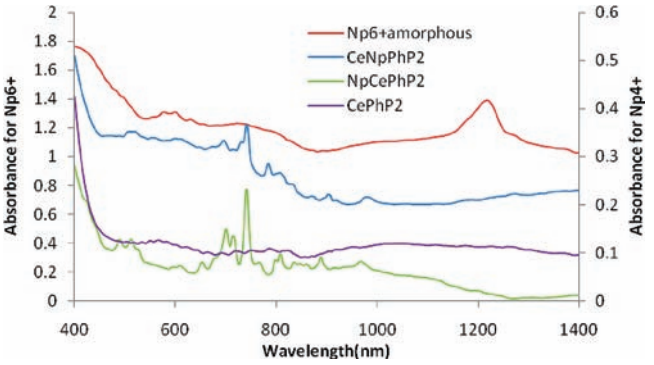

Figure 5. UV−vis−NIR spectra of Np(VI) (amorphous), $Ce[C_6H_4(PO_3H)(PO_3H_2)][C_6H_4(PO_3H)(PO_3)]\cdot 2H_2O$ (CePhP2, type I), $Np_xCe_{1-x}[C_6H_4(PO_3H)_2]_2\cdot 2H_2O$ (NpCePhP2, type II), and $Np_xCe_{1-x}[C_6H_4(PO_3H)(PO_3H_2)][C_6H_4(PO_3H)(PO_3)]\cdot 2H_2O$ (CeNpPhP2, type I), showing that there is Np(VI) in the reaction products, and Np(IV) exists in both CeNpPhP2 and NpCePhP2 crystals.

Scheme 1. Summary of Reactions of Cerium, Neptunium, and Plutonium with Phenylenediphosphonate

$$Ce^{3+} + L \xrightarrow[3d]{180^\circ C} Ce^{4-}L$$

$$Ce^{4+} + UO_2^{2+} + L \xrightarrow[3d]{180^\circ C} UO_2^{2-}/Ce^{4-}L$$

$$Ce^{3+} + UO_2^{2+} + L \xrightarrow[3d]{180^\circ C} UO_2^{2+}/Ce^{4+}L$$

$$Ce^{3+} + UO_2^{2+} + L \xrightarrow[9d]{180^\circ C} UO_2^{2+}/Ce^{4+}L + Ce^{4+}L + UO_2^{2-}L$$

$$UO_2^{2+} + NpO_2^{2+} + L \xrightarrow[3d]{180^\circ C} Np^{4+}L$$

$$UO_2^{2+} + PuO_2^{2+} + L \xrightarrow[3d]{180^\circ C} Pu^{4+}L + UO_2^{2-}/PuO_2^{2-}L$$

$$Ce^{4+} + PuO_2^{2+} + L \xrightarrow[3d]{180^\circ C} Pu^{4+}/Ce^{4+}L + PuO_2^{2+}L$$

$$Ce^{4+} + NpO_2^{2+} + L \xrightarrow[3d]{180^\circ C} Np^{4+}/Ce^{4+}L + Ce^{4+}/Np^{4-}L + Ce^{4+}L$$

$$NpO_2^{2+} + PuO_2^{2+} + L \xrightarrow[3d]{180^\circ C} Pu^{4+}/Np^{4+}L + Np^{4+}/Pu^{4-}L$$

(L=PhP2)

10:1 ratio of U/Pu and the latter clearly showing all of the f−f transitions for Pu(VI), most importantly, the main transition at 830 nm (Figure 2). EDS results are shown in Supporting Information Table S1. In Figure 3, the fluorescence spectra of $UO_2[C_6H_4(PO_3H)_2](H_2O)\cdot H_2O$ and $(U_{0.9}Pu_{0.1})O_2[C_6H_4(PO_3H)_2](H_2O)\cdot H_2O$ are shown. Energy transfer from the emission of the uranyl cations to the plutonyl cations takes place, diminishing the emission. A similar effect was observed in other heterobimetallic mixed actinide compounds.[24,25] These data point to two key features that impact other areas of plutonium chemistry. First, it gives access to Pu(VI) in a U(VI) matrix, which is useful for spectroscopic studies on Pu(VI). Second, it implies that Pu(VI) might be incorporated into uranyl alteration phases under geological conditions.

Mixing Np(VI) with Pu(VI), or either with Ce(IV), leads to the formation of both Np(VI) and Pu(VI) products and disordered heterobimetallic products containing tetravalent metals. The two possible formulas for these tetravalent compounds are

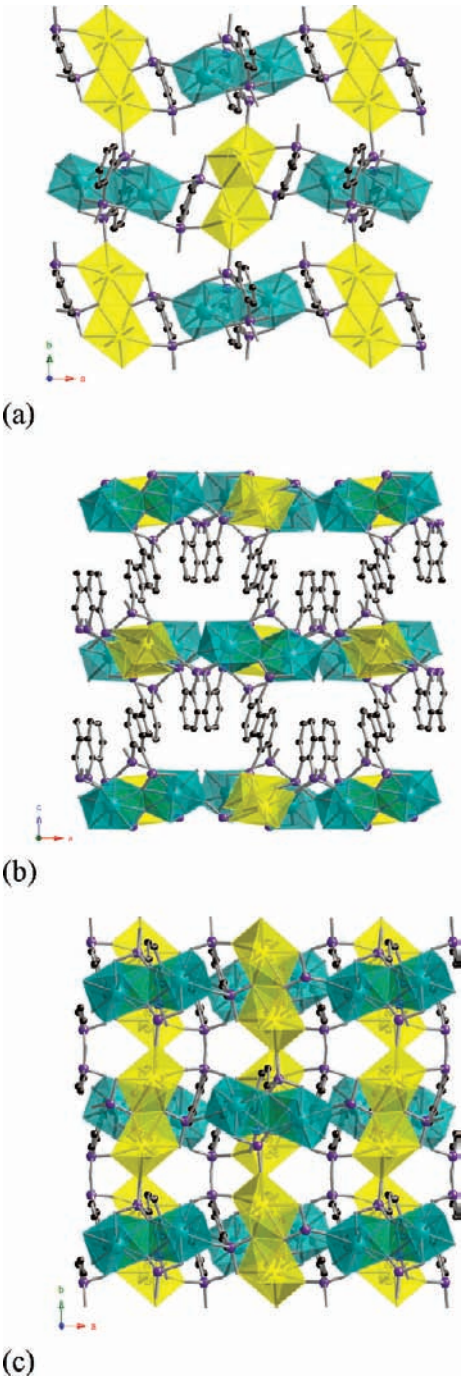

Figure 6. Depiction of the layered structure of $UO_2Ce(H_2O)[C_6H_4(PO_3)(PO_3H)]_2\cdot H_2O$ ($UO_2CePhP2$). Color Code: CeO_8 = dark green, UO_7 = bright yellow. (a) A view of part of a layer down the *a* axis showing the bonding of U(VI) and Ce(IV) dimers. (b) Relative overlap of the positions of the phenyl groups down the *b* axis. (c) The structure showing the cross overlap of the U(VI) and Ce(IV) dimers. Water molecules are omitted for clarity.

$M[C_6H_4(PO_3H)(PO_3H_2)][C_6H_4(PO_3H)(PO_3)]\cdot 2H_2O$ and $M[C_6H_4(PO_3H)_2]_2\cdot 2H_2O$ (M = Ce, U, Np, and Pu). These compounds have the same empirical formula, but the ligands are protonated differently. Both are one-dimensional structures, but the natures of the chains are different, reflecting an exquisite sensitivity to the ionic radius of metal centers given that the

dx.doi.org/10.1021/ic200006m |*Inorg. Chem.* 2011, 50, 4842–4850

Table 2. Selected Bond Distances (Å) for $UO_2Ce(H_2O)$-$[C_6H_4(PO_3H)_2]_2 \cdot H_2O$ ($UO_2CePhP2$)

bond distances (Å)			
U(1)−O(6)	2.289(5)	P(1)−O(1)	1.516(5)
U(1)−O(8)	2.372(5)	P(1)−O(2)	1.526(5)
U(1)−O(8)	2.472(5)	P(1)−O(3)	1.583(5)
U(1)−O(9)	2.495(5)	P(1)−C(1)	1.802(7)
U(1)−O(10)	2.285(5)	P(2)−O(4)	1.544(5)
U(1)−O(14)	1.773(5)	P(2)−O(5)	1.541(5)
U(1)−O(15)	1.764(5)	P(2)−O(6)	1.505(5)
Ce(1)−O(1)	2.303(5)	P(2)−C(2)	1.807(7)
Ce(1)−O(2)	2.240(5)	P(3)−O(7)	1.518(5)
Ce(1)−O(4)	2.327(5)	P(3)−O(8)	1.545(5)
Ce(1)−O(5)	2.316(5)	P(3)−O(9)	1.534(5)
Ce(1)−O(5)	2.538(5)	P(3)−C(7)	1.784(7)
Ce(1)−O(7)	2.282(5)	P(4)−O(10)	1.515(5)
Ce(1)−O(11)	2.269(5)	P(4)−O(11)	1.521(5)
Ce(1)−O(13)	2.443(5)	P(4)−O(12)	1.567(5)
		P(4)−C(8)	1.802(8)

structure type changes when the radius changes by only 0.01 Å.[28] When Pu(IV) and Np(IV) are both present in the reaction, both compounds form, and crystals of both compounds contain a 1:1 mixture of neptunium and plutonium.

While these same compounds form with Ce(IV), the cerium is not present in the same amount because a portion of the cerium is lost to the crystallization of the monometallic compound, $Ce[C_6H_4(PO_3H)(PO_3H_2)][C_6H_4(PO_3H)(PO_3)]\cdot 2H_2O$. The addition of Ce(IV) to Np(VI) and Pu(VI) provides a strong enough oxidant that a portion of the neptunium and plutonium remains in the hexavalent state. In the case of plutonium, it provides convenient access to a Pu(VI) phosphonate that we have been unable to prepare by other methods. The UV−vis−NIR spectra are shown in Figure 4. Figure 5 shows the UV−vis−NIR spectra providing evidence for the formation of an amorphous NpO_2^{2+} phase, $Ce[C_6H_4(PO_3H)(PO_3H_2)][C_6H_4(PO_3H)(PO_3)]\cdot 2H_2O$ without Np^{4+} incorporation, $Ce_{1-x}Np_x[C_6H_4(PO_3H)(PO_3H_2)][C_6H_4(PO_3H)(PO_3)]\cdot 2H_2O$, and $Ce_{1-x}Np_x\ [C_6H_4(PO_3H)_2]_2\cdot 2H_2O$. The incorporation of Ce is 15% and 14% (determined by EDS as shown in Supporting Information Table S1). Scheme 1 shows a summary of reactions of cerium, neptunium, and plutonium with phenylenediphosphonate.

Structure Descriptions of $UO_2CePhP2$, UO_2PhP2-1, UO_2-PhP2-2, UPhP2, and PuO_2PhP2. *$UO_2Ce(H_2O)[C_6H_4(PO_3)$-$(PO_3H)]_2\cdot H_2O$ ($UO_2CePhP2$).* $UO_2CePhP2$ forms a remarkable layered structure constructed from two different coordination environments for the U(VI) and Ce(IV) metal centers. The uranium atoms are contained within a classical uranyl, UO_2^{2+}, cation, and are further bound by five oxygen donors from the phosphonate ligand to create a pentagonal bipyramid, UO_7. Two UO_7 units edge-share to form a dimer. The Ce(IV) centers are found in CeO_8 dodecahedra and are ligated by both the phosphonate oxygen atoms and water. Using the Shape8 algorithm developed by Raymond and co-workers,[14b] we demonstrated that this CeO_8 adopts the D_{2d} trigonal dodecahedra geometry (Supporting Information Table 2). Again, an edge-sharing dimer is formed between two CeO_8 units. Both types of dimers are bridged by the phosphonate ligand to create layers. The two networks are interwoven, much like a cloth fabric, as shown in Figure 6a. The uranium-containing dimers are aligned approximately along the *b* axis, while the cerium dimer is almost perpendicular and orients along the *a* axis.

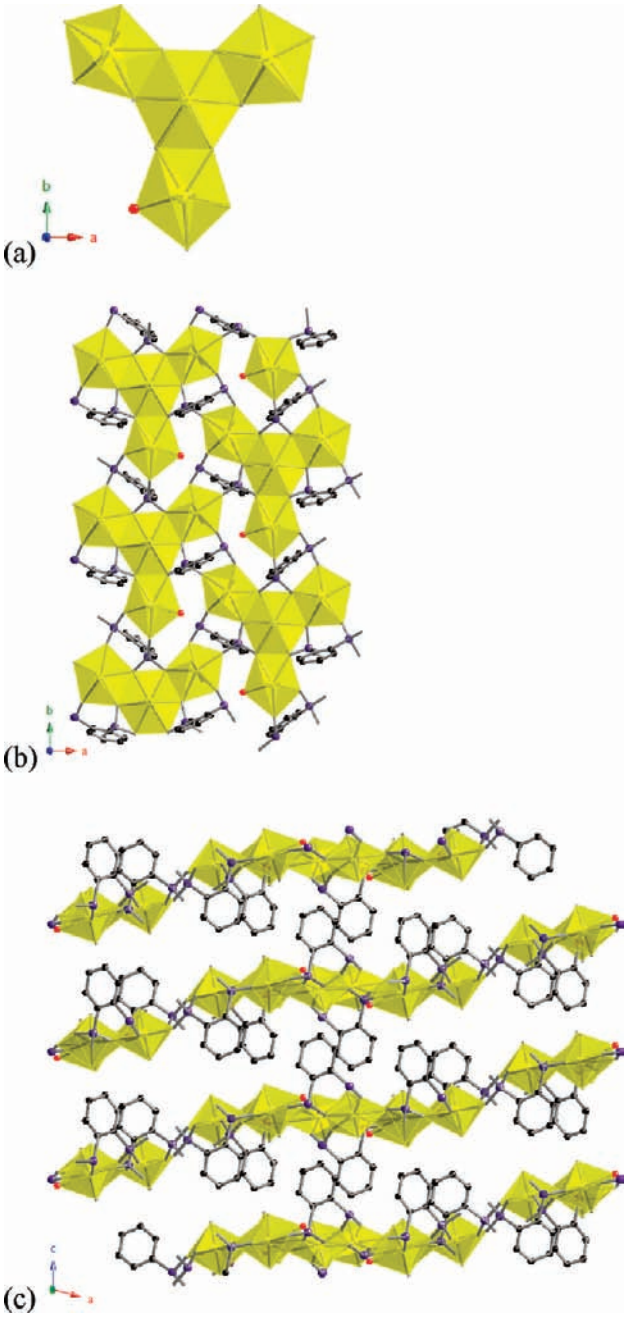

Figure 7. Depiction of the layered structure of $(UO_2)_4(H_2O)$-$[C_6H_4(PO_3H)_2][C_6H_4(PO_3H)(PO_3)]_2\cdot 5H_2O$ (UO_2PhP2-1). (a) A depiction of the topology showing a UO_8 hexagonal bipyramid surrounded by three UO_7 pentagonal bipyramids down the *c* axis. (b) The repeating unit of the layer. (c) Overview of the layered structure down the *b* aixs. Water molecules between the layers are omitted for clarity.

The uranium dimer is bonded to two PhP2 units, each chelating one of the uranium polyhedra. The uranium dimers are connected to cerium dimers by two PO_3 moieties from one PhP2 unit. The cerium dimer is bonded to four PhP2 units: two of them were used to bond to uranium dimers, while the other two are bonded only to cerium dimers. When chelating, the PO_3 unit

dx.doi.org/10.1021/ic200006m |*Inorg. Chem.* 2011, 50, 4842–4850

Table 3. Selected Bond Distances (Å) for $(UO_2)_4(H_2O)$-$[C_6H_4(PO_3H)_2][C_6H_4(PO_3H)(PO_3)]_2 \cdot 5(H_2O)$ (UO_2PhP2-1)

bond distances (Å)			
U(1)−O(19)	1.751(9)	P(1)−O(1)	1.540(9)
U(1)−O(20)	1.775(9)	P(1)−O(2)	1.537(9)
U(1)−O(15)	2.319(9)	P(1)−O(3)	1.497(9)
U(1)−O(16)	2.346(8)	P(1)−C(1)	1.802(14)
U(1)−O(14)	2.358(9)	P(2)−O(4)	1.500(9)
U(1)−O(10)	2.412(8)	P(2)−O(5)	1.504(9)
U(1)−O(17)	2.439(9)	P(2)−O(6)	1.591(10)
U(2)−O(21)	1.738(9)	P(2)−C(6)	1.800(14)
U(2)−O(22)	1.776(9)	P(3)−O(7)	1.516(9)
U(2)−O(17)	2.433(8)	P(3)−O(8)	1.555(9)
U(2)−O(2)	2.454(8)	P(3)−O(9)	1.495(9)
U(2)−O(11)	2.460(9)	P(3)−C(7)	1.824(14)
U(2)−O(1)	2.464(9)	P(4)−O(10)	1.562(9)
U(2)−O(10)	2.500(9)	P(4)−O(11)	1.550(9)
U(2)−O(18)	2.546(8)	P(4)−O(12)	1.516(9)
U(2)−P(1)	3.140(3)	P(4)−C(12)	1.814(15)
U(2)−P(6)	3.147(3)	P(5)−O(13)	1.576(9)
U(2)−P(4)	3.156(3)	P(5)−O(14)	1.500(9)
U(3)−O(24)	1.753(9)	P(5)−O(15)	1.507(9)
U(3)−O(23)	1.785(9)	P(5)−C(13)	1.796(14)
U(3)−O(9)	2.312(9)		
U(3)−O(12)	2.342(8)		
U(3)−O(1)	2.423(8)		
U(3)−O(27)	2.433(8)		
U(3)−O(18)	2.447(9)		
U(4)−O(26)	1.768(10)		
U(4)−O(25)	1.776(9)		
U(4)−O(5)	2.311(8)		
U(4)−O(7)	2.315(8)		
U(4)−O(4)	2.356(9)		
U(4)−O(2)	2.387(8)		
U(4)−O(11)	2.491(8)		

of one PhP2 moiety chelates to one metal center, while the other PO_3 unit from the same PhP2 bridges between the two metal centers. The second PhP2 ligand behaves in a similar fashion but only chelates the metal center that was not chelated by the first PhP2 moiety. Figure 6b shows the arrangement of the phenyl rings in the interlayer space. Eight phenyl rings represent a repeating unit, four from the upper layer and four from the adjacent one. Figure 6c shows the overlap of the layers along the *c* axis, illustrating that the uranium dimers and cerium dimers are interwoven. Selected bond distances are given in Table 2.

$(UO_2)_4(H_2O)[C_6H_4(PO_3H)_2][C_6H_4(PO_3H)(PO_3)]_2 \cdot 5H_2O$ (UO_2-PhP2-1). UO_2PhP2-1 also adopts a layered structure. Figure 7a illustrates the topology of UO_2PhP2-1, which contains a rare type of uranyl tetramer formed from one UO_8 hexagonal bipyramid surrounded by three UO_7 pentagonal bipyramids. This tetramer is bonded to five PhP2 units. Three of them chelate the UO_8 center using one of the PO_3 moieties while chelating the three other UO_7 units using two PO_3 moieties from the same unit. The other two PhP2's only chelate the UO_7 polyhedron. The tetramer is then connected to other tetramers through all five PhP2 units by sharing two PO_3 moieties from the same PhP2 unit. One site of the pentagonal bipyramid is occupied by water. Figure 7b illustrates the layers of UO_2PhP2-1 when viewed along the *c* axis. The repeating unit is two uranium tetramers, as shown in Figure 7c. Selected bond distances are given in Table 3.

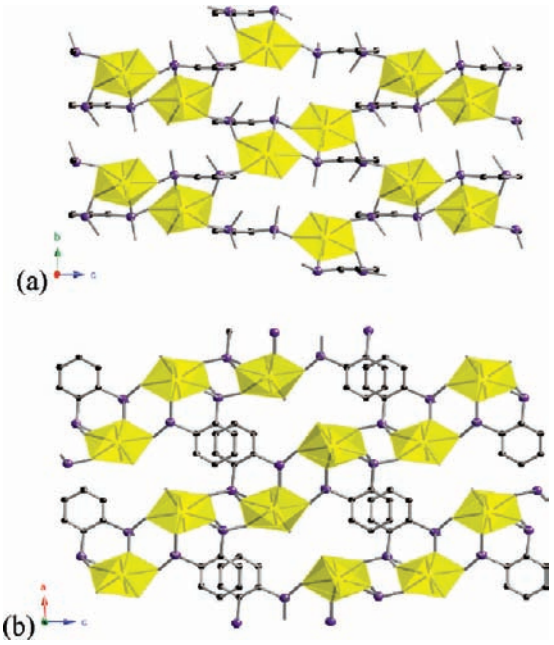

Figure 8. Depiction of the two-dimensional structure of $UO_2[C_6H_4(PO_3H)_2](H_2O) \cdot H_2O$ (UO_2PhP2-2) and $(U_{0.9}Pu_{0.1})O_2[C_6H_4(PO_3H)_2](H_2O) \cdot H_2O$ (UO_2PuO_2PhP2). (a) The layer down the *a* axis showing the bonding of U with the ligand. (b) Relative overlap of the positions of the phenyl groups down the *b* axis. Water molecules are omitted for clarity.

$UO_2[C_6H_4(PO_3H)_2](H_2O) \cdot H_2O$ (UO_2PhP2-2). UO_2PhP2-2 adopts a layered structure that contains a U(VI) pentagonal bipyramid, as shown in Figure 8a. The uranium centers are chelated by one PhP2 unit and are bonded to one adjacent polyhedron by sharing two PO_3 units from different PhP2 units, forming a pseudo-dimer. These units are then connected to two other polyhedra by one bridging PO_3 moiety. Figure 8b shows the arrangement of phenyl rings between the layers. Note that here the direction of the layer slices through the *ac* plane. There are water molecules between the layers. Selected bond distances are given in Table 4.

$U[C_6H_4(PO_3H)_2]_2 \cdot 1.5H_2O$ (UPhP2). UPhP2 provides a rare example of a U(IV) phosphonate. Only two others have been characterized by single crystal X-ray diffraction.[23,32] This compound provides a example for comparison with Ce(IV), Np(IV), and Pu(IV) counterparts. In fact, UPhP2 adopts the same topology as NpPhP2, which is different from CePhP2 and PuPhP2; the latter are isostructural with each other. Shape8 measurements show that the U(IV) and Np(IV) centers are present in a coordination environment that is best described as a square antiprism with D_{4d} symmetry. This contrasts sharply with D_{2d} trigonal dodecahedra found for Ce(IV) and Pu(IV) (Supporting Information Table 2).[28] The average U−O bond distance for UPhP2 is 2.361(6) Å and is larger than that found for NpPhP2 at 2.340(3) Å and also larger than that found for CePhP2 and PuPhP2, all of which is consistent with the actinide contraction. The selected bond distances are given in Table 5.

The UV−vis−NIR spectra here (Figure 9) demonstrate that when Np(IV) is incorporated into the $M[C_6H_4(PO_3H)(PO_3H_2)]$-

dx.doi.org/10.1021/ic200006m |*Inorg. Chem.* 2011, 50, 4842–4850

Table 4. Selected Bond Distances (Å) for $UO_2[C_6H_4(PO_3H)_2](H_2O)\cdot H_2O$ (UO_2PhP2-2)

bond distances (Å)			
U(1)−O(1)	1.7721(19)	P(1)−O(3)	1.5033(19)
U(1)−O(2)	1.7798(18)	P(1)−O(4)	1.5018(19)
U(1)−O(3)	2.3448(18)	P(1)−O(5)	1.5948(19)
U(1)−O(4)	2.3296(18)	P(1)−C(1)	1.802(3)
U(1)−O(6)	2.3364(17)	P(2)−O(6)	1.5084(18)
U(1)−O(7)	2.4045(18)	P(2)−O(7)	1.5209(19)
U(1)−O(9)	2.462(2)	P(2)−O(8)	1.5803(19)
		P(2)−C(2)	1.802(3)

Table 5. Selected Bond Distances (Å) for $U[C_6H_4(PO_3H)_2]\cdot 1.5H_2O$ (UPhP2)

bond distances (Å)			
U(1)−O(1)	2.338(6)	P(2)−O(4)	1.525(6)
U(1)−O(3)	2.290(6)	P(2)−O(5)	1.501(6)
U(1)−O(4)	2.485(6)	P(2)−O(6)	1.568(6)
U(1)−O(5)	2.348(6)	P(2)−C(2)	1.828(10)
U(1)−O(7)	2.478(6)	P(3)−O(7)	1.534(6)
U(1)−O(8)	2.347(6)	P(3)−O(8)	1.507(6)
U(1)−O(10)	2.287(6)	P(3)−O(9)	1.573(6)
U(1)−O(11)	2.316(6)	P(3)−C(7)	1.829(9)
P(1)−O(1)	1.517(6)	P(4)−O(10)	1.511(6)
P(1)−O(2)	1.578(6)	P(4)−O(11)	1.517(6)
P(1)−O(3)	1.508(6)	P(4)−O(12)	1.573(6)
P(1)−C(1)	1.815(9)	P(4)−C(8)	1.803(8)

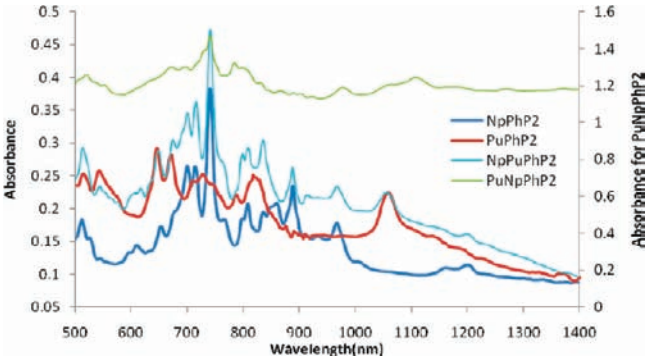

Figure 9. UV−vis−NIR spectra of $Np_xPu_{1-x}[C_6H_4(PO_3H)_2]_2\cdot 2H_2O$ (NpPuPhP2, type II) and $Pu_xCe_{1-x}[C_6H_4(PO_3H)(PO_3H_2)][C_6H_4(PO_3H)(PO_3)]\cdot 2H_2O$ (PuNpPhP2, type I), showing the incorporation of Np and Pu into each other.

$[C_6H_4(PO_3H)(PO_3)]\cdot 2H_2O$ structure type, an additional peak at 1120 nm occurs. This feature is ascribed to the Np(IV) $^4I_{9/2}\rightarrow{}^4F_{3/2}$ f−f transition. This peak was not observed in $Np[C_6H_4(PO_3H)_2]_2\cdot 2H_2O$ presumably because the D_{4d} symmetry of the Np site does not allow it to occur, whereas the lower D_{2d} geometry in $M[C_6H_4(PO_3H)(PO_3H_2)][C_6H_4(PO_3H)(PO_3)]\cdot 2H_2O$ relaxes the selection rules.

$PuO_2[C_6H_4(PO_3H)_2](H_2O)\cdot 3H_2O$ (PuO_2PhP2). PuO_2PhP2 is the first example of a Pu(VI) phosphonate. The other examples all contain Pu(IV).[23−28] The structure consists of a one-dimensional chain structure formed from PuO_7 pentagonal bipyramids containing

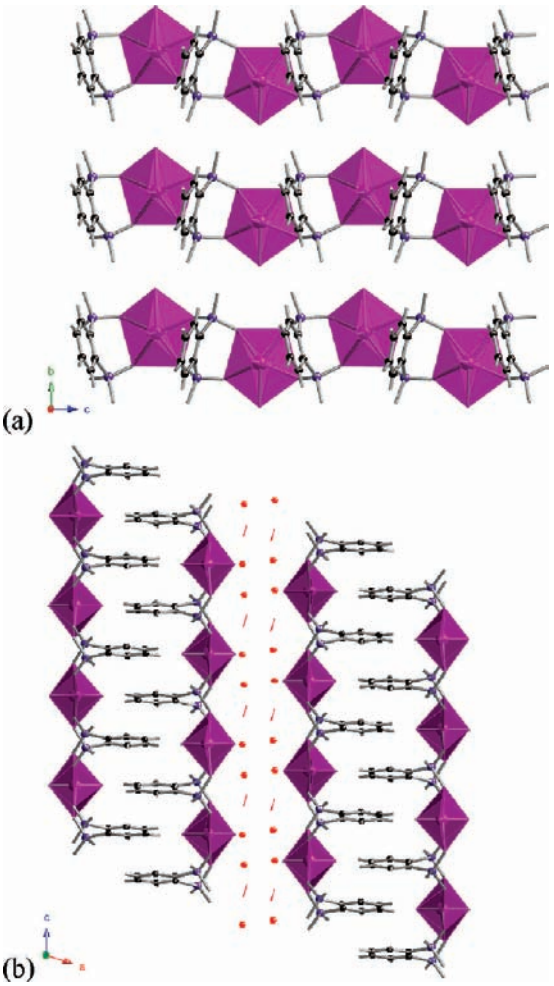

Figure 10. Depiction of the one-dimensional structure of $PuO_2[C_6H_4(PO_3H)_2](H_2O)\cdot H_2O$ (PuO_2PhP2). (a) The layer down the *a* axis showing the bonding of Pu(VI) with the ligand. Water molecules are omitted for clarity. (b) Arrangement of the phenyl groups down the *b* axis.

Table 6. Selected Bond Distances (Å) for $PuO_2[C_6H_4(PO_3H)_2](H_2O)\cdot H_2O$ (PuO_2PhP2)

bond distances (Å)			
Pu(1)−O(1)	2.341(6)	P(1)−O(1)	1.512(6)
Pu(1)−O(2)	2.364(5)	P(1)−O(2)	1.531(6)
Pu(1)−O(4)	2.385(5)	P(1)−O(3)	1.531(6)
Pu(1)−O(5)	2.346(6)	P(1)−C(1)	1.796(9)
Pu(1)−O(7)	1.731(6)	P(2)−O(4)	1.522(6)
Pu(1)−O(8)	1.725(6)	P(2)−O(5)	1.512(6)
Pu(1)−O(9)	2.474(6)	P(2)−O(6)	1.536(6)
		P(2)−C(2)	1.798(9)

PuO_2^{2+}, plutonyl cations. These polyhedra are connected to each other through the two PO_3 moieties from the same PhP2 unit. Each PhP2 unit chelates two adjacent Pu centers to extend the chain. A depiction of the chains is shown in Figure 10a. The arrangement of phenyl rings is shown in Figure 10b, with disordered water molecules between the chains. The most important data that this structure provides are the plutonyl Pu═O bond distances of 1.731(6) and 1.725(6) Å. Owing to

dx.doi.org/10.1021/ic200006m |*Inorg. Chem.* 2011, 50, 4842–4850

the actinide contraction, these distances are notably shorter than those found with U(VI) and Np(VI) and are similar to those found in $PuO_2(IO_3)_2 \cdot H_2O$.[15a] Selected bond distances are provided in Table 6.

CONCLUSIONS

In this study, we selected an exquisitely sensitive system to study the effects of mixing Ce(IV) with Np(IV), Pu(VI), and UO_2^{2+}. This investigation has yielded a number of findings that extend into other areas of actinide research. First, Ce(IV) despite having the same, or at least very similar, ionic radius as Pu(IV) does not incorporate into transuranium structures at the same levels that neighboring transuranium elements incorporate into the same structures. This can be ascribed to the much stronger oxidizing behavior of Ce(IV) than Np(IV) or Pu(IV). The Ce(IV) compounds also appear to have lower solubility than the Np(IV) or Pu(IV), and they can precipitate without incorporating transuranium elements. Second, heterobimetallic Ce(IV)/U(VI) compounds can be prepared that are unavailable with Np(IV) and Pu(IV). Our findings strongly suggest that these mixed-metal compounds are kinetic products that are not stable with respect to decomposition to monometallic compounds. This may be the reason why there are so few compounds in this class. Third, the addition of Ce(IV) to reactions containing neptunium and plutonium allows access to Np(VI) and Pu(VI) compounds that are unavailable without the presence of a strong oxidant to prevent the complete reduction of these elements to the tetravalent oxidation state. Finally, the crystallization of U(VI) compounds can act as a carrier for Pu(VI). This has important implications in the migration of plutonium from corroding used nuclear fuel where the formation of a uranyl alteration phase might mitigate the release of plutonium via incorporation in crystalline phases.

ASSOCIATED CONTENT

Supporting Information. EDS results, Shape8 results, and a crystallographic information file. This material is available free of charge via the Internet at http://pubs.acs.org.

AUTHOR INFORMATION

Corresponding Author
*E-mail: talbrec1@nd.edu.

ACKNOWLEDGMENT

We are grateful for support provided by the Chemical Sciences, Geosciences, and Biosciences Division, Office of Basic Energy Sciences, Office of Science, Heavy Elements Program, U. S. Department of Energy, under Grants DE-FG02-01ER16026 and DE-SC0002215. This material is based upon work supported as part of the Materials Science of Actinides, an Energy Frontier Research Center funded by the U.S. Department of Energy, Office of Science, Office of Basic Energy Sciences under Award Number DE-SC0001089. The SEM/EDS instrument is provided by Notre Dame Integrated Imaging Facility (NDIIF).

REFERENCES

(1) Choppin, G. R. *Radiochim. Acta* **1983**, *32*, 43–53.
(2) Albright, D.; Berkhout, F.; Walker, W. *Plutonium and Highly Enriched Uranium 1996: World Inventories, Capabilities, and Policies; Stockholm International Peace Research Institute*; Oxford University Press: New York, 1997.
(3) Wilson, P. D. *The Nuclear Fuel Cycle: From Ore to Waste*; Oxford University Press: New York, 1996.
(4) Draganic, I. G.; Draganic, Z. D.; Adloff, J.-P. *Radiation and Radioactivity on Earth and Beyond*; CRC Press: Boca Raton, FL, 1990.
(5) Clark, D. L.; Hobart, D. E.; Neu, M. P. *Chem. Rev.* **1995**, *95*, 25–48.
(6) Bhattacharyya, M. H.; Breitenstein, B. D.; Metivier, H.; Muggenburg, B. A.; Stradling, G. N.; Volf, V. *Radiat. Prot. Dosim.* **1992**, *41*, 1–49.
(7) Sutcliffe, W. G.; Condit, R. H.; Mansfield, W. G.; Myers, D. S.; Layton, D. W.; Murphy, P. W. *A Perspective on the Dangers of Plutonium*; Lawrence Livermore National Laboratory: Livermore, CA, 1995.
(8) (a) Stradling, G. N. *J. Alloys Compd.* **1998**, *271−273*, 72–77. (b) Humphreys, E. R.; Stones, V. A. *Chem. Med.* **1978**, *33*, 571–5.
(9) Brandel, V.; Dacheux, N.; Genet, M. *J. Solid State Chem.* **2001**, *159*, 39–148.
(10) Dacheux, N.; Clavier, N.; Wallez, G.; Brandel, V.; Emery, J.; Quarton, M.; Genet, M. *Mater. Res. Bull.* **2005**, *40*, 2225–2242.
(11) Dacheux, N.; Clavier, N.; Wallez, G.; Quarton, M. *Solid State Sci.* **2007**, *9*, 619–627.
(12) Dacheux, N.; Grandjean, S.; Rousselle, J.; Clavier, N. *Inorg. Chem.* **2007**, *46*, 10390–10399.
(13) Reilly, S. D.; Neu, M. P. *Inorg. Chem.* **2006**, *45*, 1839–1846.
(14) (a) Gorden, A. E. V.; Shuh, D. K.; Tiedemann, B. E. F.; Wilson, R. E.; Xu, J.; Raymond, K. N. *Chemistry* **2005**, *11*, 2842–2848. (b) Gorden, A. E. V.; Xu, J.; Raymond, K. N. *Chem. Rev.* **2003**, *103*, 4207–4282. (c) Xu, J.; Radkov, E.; Ziegler, M.; Raymond, K. N. *Inorg. Chem.* **2000**, *39*, 4156–4164. (d) Szigethy, G.; Xu, J.; Gorden, A. E. V.; Teat, S. J.; Shuh, D. K.; Raymond, K. N. *Eur. J. Inorg. Chem.* **2008**, *13*, 2143–2147.
(15) (a) Runde, W.; Bean, A. C.; Albrecht-Schmitt, T. E.; Scott, B. L. *Chem. Commun.* **2003**, *4*, 478–479. (b) Bean, A. C.; Scott, B. L.; Albrecht-Schmitt, T. E.; Runde, W. *Inorg. Chem.* **2003**, *42*, 5632–5636.
(16) Brandel, V.; Dacheux, N. *J. Solid State Chem.* **2004**, *177*, 4743–4754.
(17) Brandel, V.; Dacheux, N. *J. Solid State Chem.* **2004**, *177*, 4755–4767.
(18) Dacheux, N.; Podor, R.; Brandel, M.; Genet, M. *J. Nucl. Mater.* **1998**, *252*, 179–186.
(19) (a) Nash, K. L. *J. Alloys Cmpd.* **1997**, *249*, 33–40. (b) Jensen, M. P.; Beitz, J. V.; Rogers, R. D.; Nash, K. L. *J. Chem. Soc., Dalton Trans.* **2000**, *18*, 3058–3064. (c) Chiarizia, R.; Horwitz, E. P.; Alexandratos, S. D.; Gula, M. J. *Sep. Sci. Technol.* **1997**, *32*, 1–35.
(20) Gorman-Lewis, D.; Elias, P.; Fein, J. B. *Environ. Sci. Technol.* **2005**, *39*, 4906–4912.
(21) Fowle, D. A.; Fein, J. B.; Martin, A. M. *Environ. Sci. Technol.* **2000**, *37*, 3737–3741.
(22) Bray, T. H.; Nelson, A.-G. D.; Jin, G. B.; Haire, R. G.; Albrecht-Schmitt, T. E. *Inorg. Chem.* **2007**, *46*, 10959–10961.
(23) Nelson, A.-G. D.; Bray, T. H.; Zhan, W.; Haire, R. G.; Albrecht-Schmitt, T. E. *Inorg. Chem.* **2008**, *47*, 4945–4951.
(24) Nelson, A.-G. D.; Bray, T. H.; Albrecht-Schmitt, T. E. *Angew. Chem., Int. Ed.* **2008**, *47*, 6252–6254.
(25) Nelson, A.-G. D.; Bray, T. H.; Stanley, A. F.; Albrecht-Schmitt, T. E. *Inorg. Chem.* **2009**, *48*, 4530–4535.
(26) Diwu, J.; Nelson, A.-G. D.; Albrecht-Schmitt, T. E. *Comment Inorg. Chem.* **2010**, *31* (1&2), 46–62.
(27) Diwu, J.; Nelson, A.-G. D.; Wang, S.; Campana, C. F.; Albrecht-Schmitt, T. E. *Inorg. Chem.* **2010**, *49*, 3337–3342.
(28) Diwu, J.; Wang, S.; Liao, Z.; Burns, P. C.; Albrecht-Schmitt, T. E. *Inorg. Chem.* **2010**, *49*, 10074–10080.
(29) Reiter, S. A.; Assmann, B.; Nogai, S. D.; Mitzel, N. W.; Schmidbaur, H. *Helv. Chim. Acta* **2002**, *85*, 1140–1150.
(30) Sheldrick, G. M. *Acta Crystallogr.* **1995**, *A51*, 33–38.
(31) Sheldrick, G. M. *Acta Crystallogr.* **2008**, *A46*, 112–122.
(32) Grohol, D.; Clearfield, A. *J. Am. Chem. Soc.* **1997**, *119*, 4662–4668.